THE ASTROPHYSICAL JOURNAL, 315:154–161, 1987 April 1

TWO BINARY CYCLES OF GX 301−2

RICHARD E. ROTHSCHILD AND YANG SOONG
Center for Astrophysics and Space Sciences, University of California, San Diego
Received 1986 April 17; accepted 1986 September 22

ABSTRACT

The slow X-ray pulsar, GX 301−2, has been observed throughout two full binary cycles of 41.5 days in the energy range 13–170 keV by the UCSD/MIT Hard X-Ray and Low Energy Gamma-Ray Experiment aboard *HEAO 1*. Increased intensity and variability was observed for about 4 days near periastron during the two binary cycles, which were separated by 6 months in 1978. The spectral shape was not observed to vary with binary phase, with the possible exception of a steepening of the continuum above 20 keV near superior conjunction in one of the two observing epochs. Evidence for a spectral line was found in the data at the 1% confidence level, but not confirmed in the remaining data. The temporal variability of GX 301−2 was not consistent with simple models of X-ray production by interaction of the stellar wind with the neutron star, implying that future modeling must include effects on wind density and speed caused by shocks in the wind, the X-ray flux from the neutron star, the gravitational influence of the neutron star, and possible mass accumulation near the neutron star.

Subject headings: pulsars — stars: winds — X-rays: binaries — X-rays: spectra

I. INTRODUCTION

The object GX 301−2 is a slow X-ray pulsar in a binary system consisting of an early-B emission-line star (WRA 977) and a neutron star. White and Swank (1984 and references therein) have used the 700 s pulsar variability to determine the orbital parameters of the system. These include an orbital period of 41.5 days, eccentricity of 0.475, and a longitude of periastron of −49°. This system also exhibits a dramatic increase in X-ray flux that lasts for about 4 days every 41.5 days below 20 keV. In this same energy range Makino, Leahy, and Kawai (1985) report a significantly shorter duration of bright flux (<1 day, but this may have been a single flare and not the entire period of enhanced flux), while Warwick, Watson, and Sims (1981) describe this duration as lasting from 5 to 10 days. The centroid of this 2–20 keV flaring occurs 1.2 ± 0.8 days before periastron, as determined from the *Ariel 5* and *SAS 3* timing data (White and Swank 1984).

Models using a simple stellar wind from the primary along with derived orbital parameters have been somewhat successful in predicting the binary phase dependence of the observed flux (White and Swank 1984; Watson, Warwick, and Corbet 1982; and Kelley, Rappaport, and Petre 1980). Most models, however, have explained neither the short duration of the bright levels near periastron nor the occurrence of the centroid of the bright levels before periastron.

II. OBSERVATIONS

GX 301−2 was scanned by the UCSD/MIT Hard X-Ray and Low Energy Gamma-Ray Experiment (Matteson 1978) aboard *HEAO 1* for ~41 days in the beginning and middle of 1978. These instruments contained two low energy phoswich scintillators (LEDs) that were sensitive to X-rays in the 13–170 keV range. The LEDs had slat-collimated fields of view of $1^\circ.2 \times 20^\circ$ oriented at 30° to the spacecraft scan plane and comprised about 100 cm^2 of effective area each. The results from LED1 were not used, due to source confusion, and only results from LED2 will be reported here. Since the ecliptic longitude of the *HEAO 1* scan plane increased 1° per day, the collimator design made scanning observations of a given source (denoted as an epoch) possible for 2 weeks or more depending on the ecliptic latitude of the source. In the case of GX 301−2, this source was viewed throughout a complete binary cycle in each of two scanning epochs.

III. RESULTS

a) Light Curves

Figure 1 shows the scan-by-scan, background-subtracted intensities of GX 301−2 in early 1978 (second epoch) and mid-1978 (third epoch) that have been corrected for collimator response. The time between individual scans is about 33 minutes, and gaps in the data are due to Earth occultations, South Atlantic Anomaly passages, pointing observations (especially evident in the third epoch), and data rejected for reasons of quality. In both 41.5 day epochs, the brightening near periastron is quite apparent, as is the generally constant flux away from periastron. One instance of flaring outside of periastron passage is seen just before JD 2,443,525.

Figure 2 shows the "bright" level near periastron passage in the second and third epochs plotted versus binary phase (JD $2{,}443{,}450.0 + 41.51E$; White and Swank 1984). The approximate centers of the "bright" levels can be determined by computing the count rate–weighted phases, and they are 0.981 (JD 2,443,532.20) and 0.969 (JD 2,443,739.23) for the second and third epochs, respectively. The value obtained for the center of the second epoch "bright" level is a more reliable measure of the center of the activity since the coverage is more complete than in the third epoch. These results are consistent with the mean value of 0.971 ± 0.019 (1.2 ± 0.8 days before periastron) quoted by White and Swank (1984) for the phase of the centroid of the enhanced flux in the 2–20 keV range.

The high degree of variability of the "bright" level from scan to scan is evident, with the most intense point almost 25 times the quiescent rate, and with factor of 2 changes within a half hour not uncommon. Stellar wind models of eccentric X-ray binaries, such as GX 301−2, predict a smooth increase and

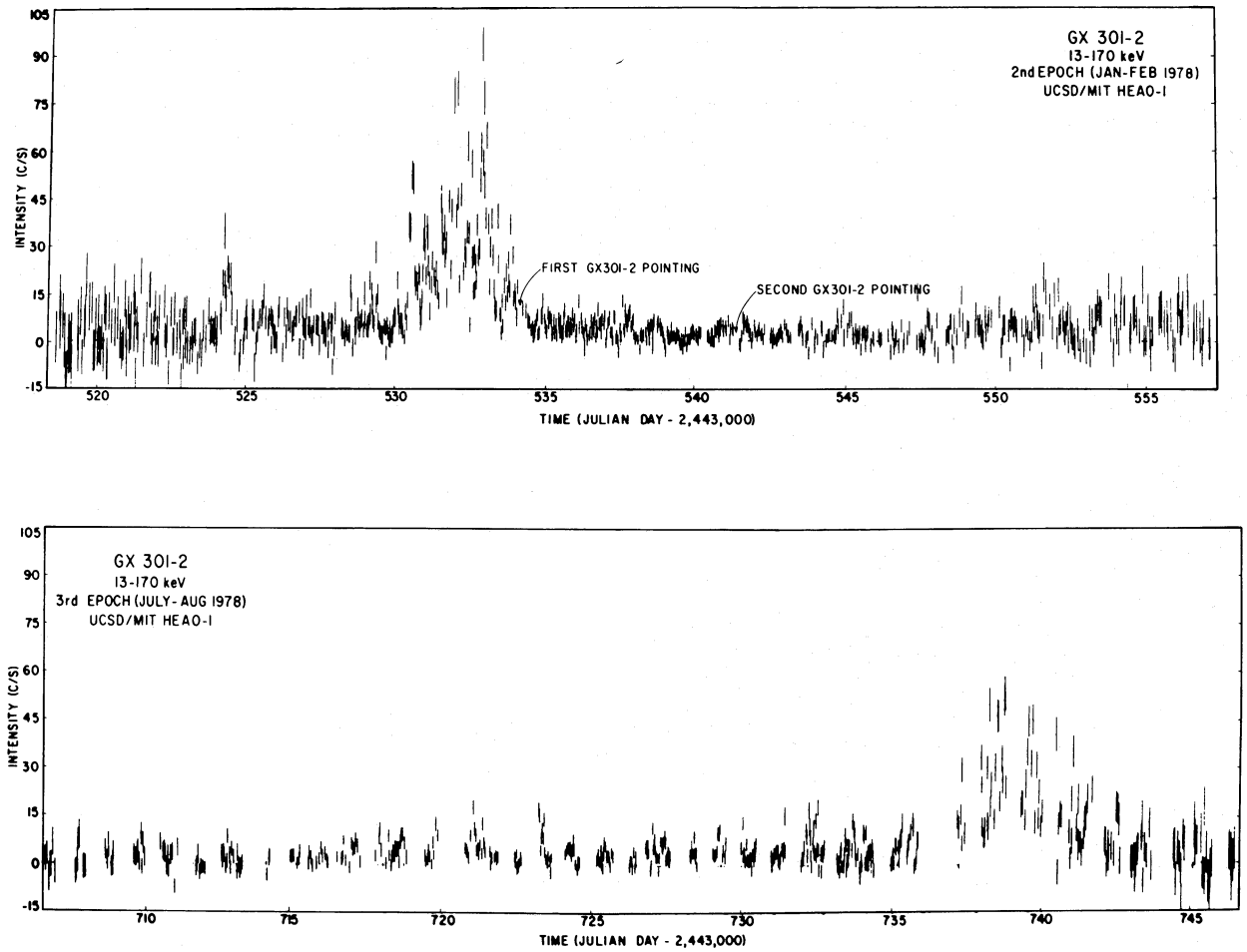

FIG. 1.—The 13–170 keV count rate from GX 301−2 vs. time in days for two epochs in 1978. Each data point is the mean rate over the 10–15 s exposure to the source each revolution of the *HEAO 1* spacecraft. The scans are multiples of 33 minutes apart. The data have been corrected for aperture response and background count rate. The two *HEAO 1* pointed observations of this source are marked.

then decrease in X-ray flux as the neutron star passes through periastron (see § III). The variability in both GX 301−2 epochs may then be characterized as a smooth rise and fall of up to a factor of ~4 on which faster, more chaotic variations of larger amplitude are superposed. On the other hand, a superposition of just randomly occurring flares (i.e., shot noise behavior) might also account for the observed variability. Given the statistical uncertainties we cannot rule out similar flaring increases of an order of magnitude or less away from periastron. The 700 s X-ray pulsar variability has not been removed. Our observations of these pulsations during the two pointing episodes (see Fig. 1) in the second epoch show that pulsar activity accounts for 50% variations when the mean rate is low. If the pulse amplitude is similar at higher rates, the bulk of the observed variability seen in Figure 2 must be attributed to true variability in the X-ray emission from the neutron star.

When the individual scans comprising the entire two epochs are combined into bins of 0.83 days (50 bins per binary period), the scan-to-scan variability, especially near periastron, is lost, but the general appearance of the binary light curve becomes more apparent (see Fig. 3). In both epochs the mean intensity away from periastron is the same, ~4 counts per second; the peak intensities are similar, ~36 counts per second; and the duration of the bright levels are the same, ~4 days. Lower intensities were observed in both epochs near days JD 2,443,540–2,443,545 and JD 2,443,709–2,443,714, respectively, which were about 10 days after periastron passage. This is the phase interval where an eclipse would have occurred if the GX 301−2 system's inclination were larger. The third epoch values follow the periastron passage predicted for JD 2,443,699.0, just before our observations began.

The data from the two epochs have been combined into a single folded light curve with 4.15 day bins for spectral accumulations (see § III*b*). The occurrence of zero phase has been increased by 1.15 days ($\Delta\phi = 0.028$) to JD 2,443,451.15 in order to center the "bright" level in a single phase bin ($0.9 < \phi < 1.0$). The observed count rate from 13–40 keV is displayed in Figure 4. Due to the coincidental phasing of the 41.5 day orbital period of GX 301−2 and the 6 month separation between scanning epochs by *HEAO 1*, all phase bins in Figure 4 have approximately the same uncertainty in their weighted mean values. The factor of 2 decrease in intensity around binary phase 0.2 (where an eclipse would occur if the system inclination were larger) is clearly defined, as is a second minimum near binary phase 0.7. Note that phases are with respect to the mean anomaly, which differ greatly from phases based upon true anomaly, since the orbit of GX 301−2 is significantly eccentric. The intensities from the two observing epochs suggest that the general shape of the light curve is stable on time scales of one-half year.

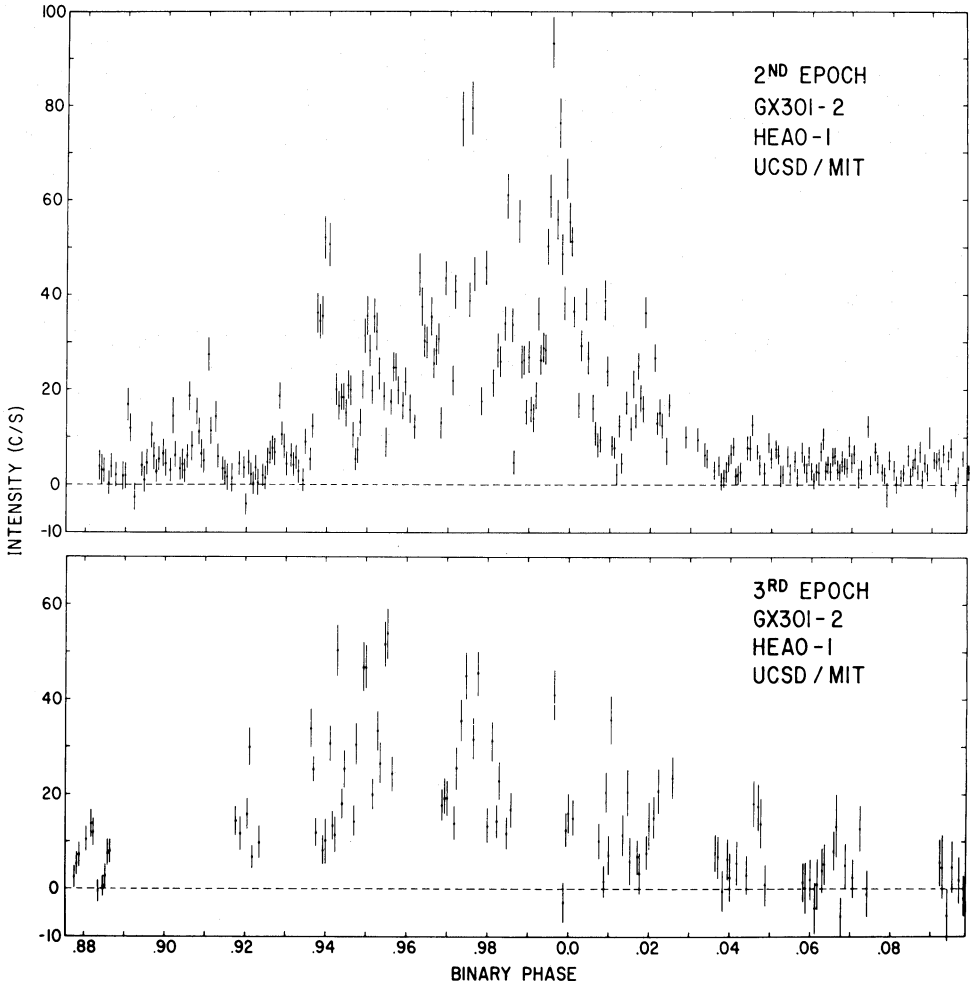

FIG. 2.—The 13–170 keV count rate from GX 301 − 2 vs. binary phase for the periods of enhanced intensity visible in Fig. 1. The points represent the average count rate for each scan over the source, and the phase is with respect to JD 2,443,450.0 + 41.51*E*.

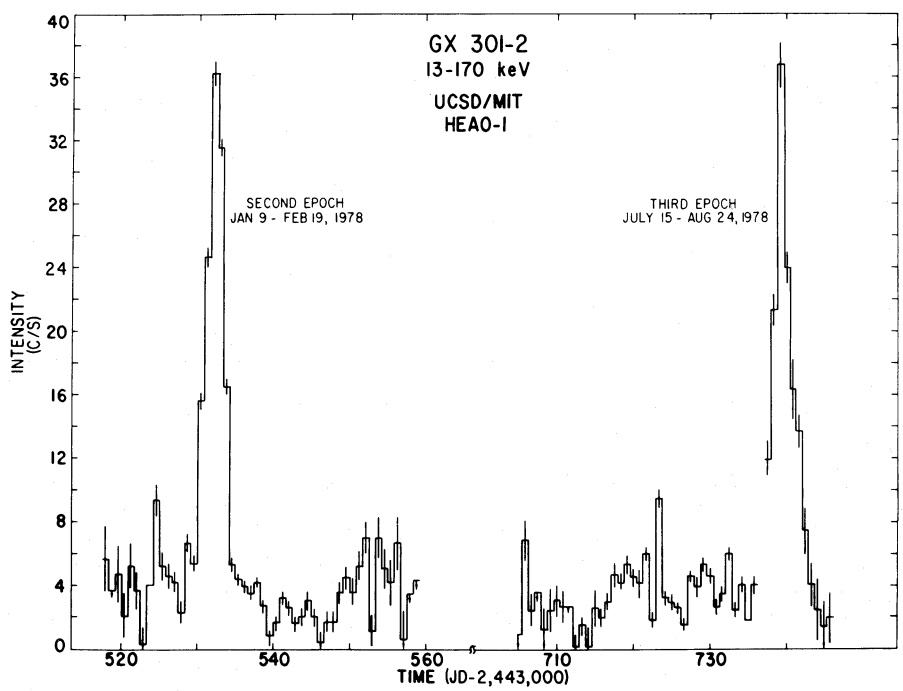

FIG. 3.—The 13–170 keV count rate from GX 301 − 2 vs. time in days for the two epochs in 1978. The bin width is 0.83 days.

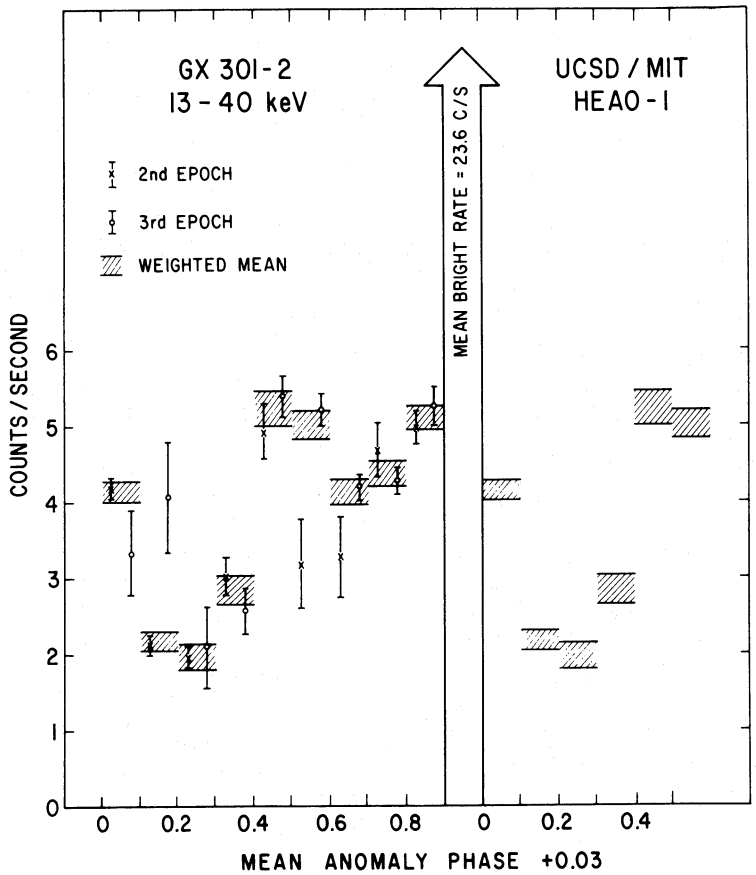

FIG. 4.—The observed count rate from 13 to 40 keV from GX 301−2 for both *HEAO 1* observing epochs folded on 41.51 day period (phase zero occurrence is at JD 2,443,450.0 + 1.15). The 0.028 phase shift centered the "bright" level in the 0.9–1.0 phase bin for subsequent spectral analysis. The hatched areas represent $\pm 1\ \sigma$ for the weighted mean of the second epoch (*crosses*) and third epoch (*open circles*) values. The shape of the light curve is the same in the two epochs at the 99% confidence level.

To summarize the temporal variability of GX 301−2, three regions of different intensity are indicated: (1) the "bright" region near periastron that lasts about 10% of the binary period and is centered about binary phase 0.98; (2) the "low" region lasting 10%–20% of the binary period centered near phase 0.2; and (3) the rest, including a second smaller minimum, which constitutes the "mean" level. This description holds for both binary periods separated by 6 months. The "bright" region may further be described as either (*a*) the sum of a smoothly varying component that increases to about 4 times the "mean" level and then decreases with superposed flaring activity that can cause additional factor of 5 variations on time scales of hours, or (*b*) entirely composed of randomly occurring flares accounting for more than an order of magnitude increase in intensity on time scales of hours. The flux level of the "mean" region is about 8×10^{35} ergs s^{-1} from 13 to 170 keV assuming a distance of 1.8 kpc (Parkes *et al.* 1980).

b) *Spectral Shape Variations*

The 13–170 keV count rate spectra of GX 301−2 from the two scanning epochs were accumulated separately in the 4.15 day bins of Figure 4. Directly comparing the two count rate spectra of each epoch for a given phase bin allows for tests for variability in spectral shape that do not depend upon the specific form of the spectral model. From 21 to 68 keV the "bright," periastron spectra were identical ($\chi^2 = 4.4$ for 6 degrees of freedom; probability of being exceeded by chance, P, is 0.7), but if one includes the data down to 13.5 keV, the comparison is poor ($\chi^2 = 26.1$ for 9 degrees of freedom, $P = 0.002$). Hence, the spectra of the "bright" region are identical in mean intensity and spectral shape above 21 keV. Below 21 keV, however, the second epoch data is 19% brighter than that from the third epoch. The 21–68 keV data could not have been 19% brighter ($\chi^2 = 55.8$ for 6 d.o.f.). This difference may be attributable to different values of average circumstellar photoelectric absorption at these two times (e.g., Swank *et al.* 1976), or may be due to a difference in X-ray production at the neutron star. Both Swank *et al.* (1976) and White and Swank (1984) display X-ray spectra with such low energy variability.

The "low" (phases 0.1–0.3) and "mean" (phases 0.0–0.1 and 0.3–0.9) region spectra were accumulated in each epoch. These count rate spectra were compared as the "bright" ones were above. The 13.5–68 keV comparison of "mean" count rate spectra yielded a $\chi^2 = 15.3$ for 9 degrees of freedom ($P = 0.08$). This indicates that the average intensity and spectral shape were identical within experimental uncertainties. Due to the lower intensity, a meaningful comparison of the "low" count rate spectra could only be done between 13.5 and 41 keV. In this range the two epoch's spectra were dissimilar ($\chi^2 = 94.3$ for 7 degrees of freedom, $P < 10^{-6}$). The disagreement occurs above 21 keV with epoch 3 brighter than epoch 2.

A comparison was also made between the "mean" and

"low" levels of each epoch to determine if a significant spectral difference between them existed. This was done by taking the ratio of count rates, energy bin by energy bin, and testing against the hypothesis of a constant ratio. In the early 1978 epoch, the "low" level occurred near the peak of the collimator response, whereas the mid-1978 "low" level occurred early in the epoch when the sensitivity was lower. This fact affected the statistical significance of the two comparisons. The early 1978 epoch "low-mean" comparison yielded a χ^2 of 23.6 for 8 degrees of freedom from 13.5 to 54 keV, which is equivalent to a difference in spectral shape at the $P = 0.003$ level. The largest deviations from a constant hypothesis occurred above 25 keV and implied that the "low"-level spectrum was steeper above 25 keV than the "mean" level spectrum. The mid-1978 comparison showed no significant steepening of the "low" phase ($\chi^2 = 7.9$ for 7 d.o.f.). This is consistent with the direct comparison of "low" data that showed the epoch 3 data above 21 keV to be relatively brighter than the epoch 2 data, while comparisons of the "mean" data showed no difference.

The possible hardening of the second epoch "low" spectrum above 21 keV was also tested by examining the hardness ratio of counts, R = 13.5–25 keV/25–41 keV. A relative steepening would be seen as an increase in R. Table 1 shows R for the "bright", "mean", and "low" levels for each epoch. This ratio is seen to be essentially identical within experimental uncertainties for five of the six spectra. Only the "low" level in epoch 2 is significantly different. Further observations above 20 keV will be necessary to determine if the epoch 2 result is a repeating phenomenon.

c) *Spectral Parameter Variations*

The incident spectrum can be represented as a power law of photon index Γ up to a cutoff energy E_c, above which it becomes an exponential of characteristic energy E_F. The GX 301−2 spectra were fitted by passing the model through the detector response to form a model count rate spectrum which was compared to the observed count rate spectrum via a χ^2 test. Parameters of the model were simultaneously varied to minimize χ^2. The best-fit model was then used to generate counts-to-photons efficiencies, and thereby to create the inferred incident photon spectrum. The results for fitting for Γ have little quantitative value, since only the lower few energy channels constrain the best-fit values. The power-law index must be included in the fitting process, however, since it affects the values of E_c and E_F due to the energy resolution of the scintillator (23% at 60 keV).

The fitted parameters for the spectra in the seven phase bins comprising the "mean" level in both epochs were consistent with the same characteristic energy, 7.55 keV ($\chi^2 = 8.2$, 13 d.o.f., $P = 0.83$), the same cutoff energy, 24.44 keV ($\chi^2 = 22.2$, 13 d.o.f., $P = 0.052$), and the same power-law index, 1.50 ($\chi^2 = 22.5$, 13 d.o.f., $P = 0.048$). A single "mean" level spectrum was then accumulated for each epoch, and the best-fit parameters are given in Table 2. These parameters are consistent with the average values given above. Similarly, the fitted parameters for the spectra in the two phase bins comprising the "low" level in both epochs were consistent with characteristic energy, 3.27 keV ($\chi^2 = 0.40$, 3 d.o.f., $P = 0.94$); cutoff energy, 23.31 keV ($\chi^2 = 1.76$, 3 d.o.f., $P = 0.62$); and power-law, 0.93 ($\chi^2 = 3.07$, 2 d.o.f., $P = 0.21$). Fitting for one of the values of the power-law index in the second epoch did not converge to a meaningful result (-8.37 ± 1.31), and it was not used in the above calculation. A single "low"-level spectrum was accumulated from the two spectra in each epoch, and the best-fit parameters are given in Table 2. These parameters also are consistent with the average values expressed above. Finally, the "bright" level best-fit parameters are given in Table 2. They are consistent with a characteristic energy of 8.04 keV, a cutoff energy of 21.64 keV, and a power-law index of 0.56.

While all six spectra represented in Table 2 (and shown in Fig. 5) are quite similar, the "bright" level spectra may tend to cutoff at slightly lower energy and have a slightly flatter power-law index. Based on model fitting, as contrasted to comparing observed counts, the "low"-level spectra may become steeper above the cutoff energy. This steepening, we feel, cannot be claimed as significant, since it did not appear in both "low" count data sets. Hence, we find no compelling evidence for spectral variability around the binary orbit of GX 301−2 on 4 day time scales.

TABLE 1

COUNT RATE HARDNESS RATIOS FOR GX 301−2

Epoch	R[a]
2:	
Bright	3.55 ± 0.09
Mean	3.05 ± 0.18
Low	6.01 ± 1.12
3:	
Bright	3.50 ± 0.17
Mean	3.17 ± 0.14
Low	2.67 ± 0.79

[a] $R = \frac{13.5\text{–}25 \text{ keV}}{25\text{–}41 \text{ keV}}$

TABLE 2

SPECTRAL PARAMETERS OF GX 301−2

Epoch	Γ	E_c(keV)	E_F(keV)	$\chi^2/13$[a]
2: Bright	0.49 ± 0.18	21.3 ± 0.5	8.2 ± 0.3	28.0
Mean	1.32 ± 0.22	25.2 ± 1.5	8.0 ± 1.1	21.5
Low	1.05 ± 0.40	24.6 ± 2.0	3.0 ± 1.9	5.6
3: Bright	0.68 ± 0.23	22.5 ± 0.8	7.4 ± 0.6	6.1
Mean	1.46 ± 0.15	25.3 ± 1.2	7.4 ± 0.9	8.0
Low	0.46 ± 1.04	25.7 ± 3.3	2.7 ± 4.2	20.9

[a] χ^2 for 13 degrees of freedom.

d) *Spectral Features*

At the suggestion of Jean Swank, we investigated the possibility of the existence of hard X-ray spectral lines that might be interpreted as cyclotron features. As seen in Table 2, the second epoch "bright" spectrum χ^2 per degree of freedom exceeded 2. Adding an unresolved emission line to the model yielded an improved χ^2 of 12.1 for 11 degrees of freedom. Adding an absorption line instead gave χ^2 of 11.0 for 11 degrees of freedom. The F-test reveals this to be significant at the 1% level. The emission line was at 30.5 ± 0.5 keV with intensity of $(1.0 \pm 0.3) \times 10^{-2}$ photons cm^{-2} s^{-1}, and the absorption line was at 23.8 ± 0.3 keV with equivalent width of 1.3 ± 0.3 keV. Since the emission-line energy is very near the iodine K-edge energy (33.17 keV), one must be careful to include the ~4% drop in response just above this energy in the detector response calculations. We have measured the shape of the response as a function of energy at the Stanford Synchrotron

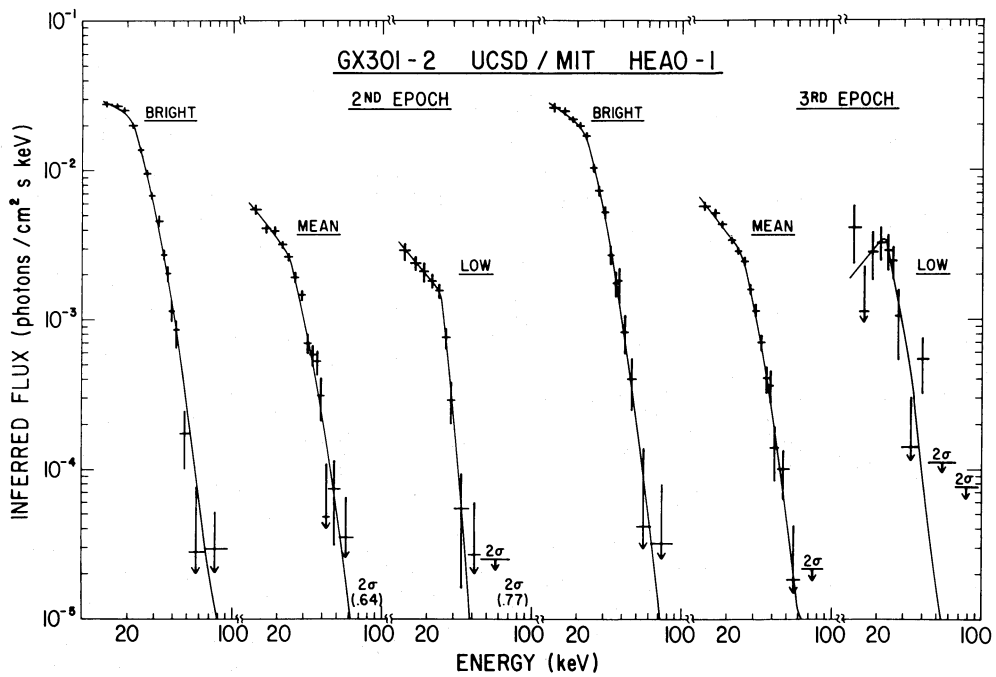

FIG. 5.—The "bright" ($0.9 < \phi < 1.0$), "mean" ($0.0 < \phi < 0.1$ and $0.3 < \phi < 0.8$), and "low" ($0.1 < \phi < 0.3$) spectra of GX 301−2 for both *HEAO 1* observing epochs. The solid lines are the best-fit spectra, as described in the text. All error bars are 1 σ, and upper limits are 2 σ.

Radiation Laboratory, and this effect is included in our detector response calculation.

Testing of the other five spectra for lines at those energies yielded no confirmation of this result. An absorption line, significant at $\sim 3\%$, was fitted in the second epoch "mean" level spectrum at 21.4 ± 0.6 keV with equivalent width of 1.1 ± 0.3 keV. Since, however, we were unable to confirm any of these lines within our data, we view this as a tantalizing result that will merit investigation by future hard X-ray missions.

We can summarize the spectral variations of GX 301−2 as follows. The spectral shape is generally constant in time. The spectral shapes are the same, within experimental uncertainty, from two epochs separated by 6 months, and throughout a given binary cycle, with the possible exception near phase 0.2. There the flux drops by a factor of 2, and the continuum possibly steepens temporarily. The spectral parameters derived here are consistent with those found by White and Swank (1984). Even though the light curves may indicate flaring and/or smooth variations near periastron, the spectrum taken there is essentially no different than that seen in the "mean" level.

III. DISCUSSION

The relevant features of the binary light curve of GX 301−2 are as follows:

1. The "bright" level duration is $\sim 10\%$ of the binary period.
2. The "bright" level is centered near phase 0.98.
3. On a daily average, the "bright" level maximum intensity is 10 times the "mean" level.
4. A factor of 2 drop in intensity occurs near phases 0.1–0.3.
5. A second smaller minimum repeats near phase 0.7.
6. The spectral shape does not vary with binary phase, except possibly near phase 0.2.
7. The "mean" level is 8×10^{35} ergs s^{-1} from 13 to 170 keV.
8. The "bright" level is characterized by hour time scale large variations in intensity that may or may not also be superposed upon a factor of 4 rise and then fall in intensity. These characteristics must be addressed in any attempts to model this system.

We constructed a wind-accretion model of GX 301−2 along the lines of Okuda and Sakashita (1977), assuming the binary parameters determined from pulsed data (White and Swank 1984 and references therein), from optical observations of WRA 977 (Parkes *et al.* 1980), and models of the wind from bright main-sequence stars (Barlow and Cohen 1977; Castor, Abbott, and Klein 1975). The model ignores the effects of both the X-rays and the gravitational field of the neutron star on the character of the wind, assumes no storage of matter near the neutron star, but does calculate the line-of-sight attenuation of X-rays through the wind (Robinson-Saba 1983), due to Compton scattering and photoelectric absorption. To take these latter two effects into account, we have calculated the line-of-sight electron density (Barlow and Cohen 1977) for the Compton scattering, and we selected an optical depth at the stellar surface as a free parameter that was then combined with the electron density to produce an equivalent optical depth for photoelectric absorption. This equivalent optical depth for photoelectric absorption makes no assumptions as to the ionization state or chemical composition of the wind, or at what energy the absorption takes place. It is just an optical depth that scales around the orbit with the line-of-sight electron density. Hence, when comparing results to other energy ranges in a consistent manner, one must take the above factors into account. The wind velocity law was chosen to have a simple $[1 - (R_*/r)]^\alpha$ form, with α as a free parameter, where R_* is the stellar radius and r is the radial distance from the center of the star.

Several attempts to reproduce the temporal characteristics of GX 301−2 revealed that no single set of parameters can accurately describe all of them. For instance, the peak in the "bright" level could be made to occur before periastron if one used four optical depths at the stellar surface and very low wind speeds, independent of the wind speed exponent. The observed "mean" flux in this case, however, was at least a factor of 5 too low (assuming 100% conversion of mass flux to X-ray flux), the flux at phase 0.25 essentially disappeared, and most significantly, the width of the "bright" level exceeded observations. On the other hand, the "bright" level width was satisfactory as was the factor of 2 dip in intensity for higher (and probably more appropriate) wind speeds and lower line-of-sight absorption, but the peak of the "bright" level no longer occurred before periastron and its intensity as compared to the "mean" level was an order of magnitude too large. More than one X-ray emission region (e.g., addition of an extended X-ray corona) was not considered since the spectrum was essentially invariant, indicative of a single dominant emission region. Consequently, any attempt to derive meaningful parameters of the stellar wind from modeling the GX 301−2 X-ray variations must await more detailed descriptions of the wind speed and the interaction of the wind with the X-ray flux (see Friend and Castor 1982; MacGregor and Vitello 1982). A similar conclusion was reached by Warwick, Watson, and Sims (1981) and White and Swank (1984).

The factor of 2 drop in intensity near phase 0.2 cannot be purely a complete occultation of a portion of the X-ray emission region by the main-sequence star. The duration of the dip implies an obscuring region greater than 0.4 AU, which is also the periastron distance. Hence, the wind region within one or two stellar radii of the primary must be about 10^{24} atoms cm^{-2}, or dense enough to cause the intensity drop by Compton scattering. Swank *et al.* (1974) quoted values consistent with 10^{24} atoms cm^{-2} for lower energy observations of GX 301−2. The second minimum in the light curve near mean anomaly phase 0.7 cannot be due to some kind of occultation of the primary by the neutron star, since inferior conjunction occurs at mean anomaly phase 0.96. Mean anomaly phase 0.7 is, however, approximately when the neutron star is moving directly toward Earth. Perhaps matter accumulates (in a shock?) in front of the neutron star as it orbits in the wind, and this matter is dense enough to cause the second minimum.

An alternative approach to the larger question of GX 301−2 variability has been described by Boyle (1984) and Brown and Boyle (1984) in which they attempt to model the temporal variability of eccentric X-ray binaries using the modulation of mass transfer through a "Roche lobe" nozzle near the inner Lagrangian point. They find that a dynamic variation in the mass transfer rate, $\dot{M}$, will result from variations in binary separation. They have been able to reproduce the 10% duration of the bright level in GX 301−2. They further find that the instantaneous value of $\dot{M}$ affects the motion of the effective Roche lobe in such a way as to allow the maximum in $\dot{M}$ through the nozzle to occur before periastron under certain conditions (not necessarily the same conditions that gave rise to the preferred "bright" level duration). Whether or not this model can predict the centroid of the bright X-ray flux occurring before periastron will depend upon the details of the mass transfer from the nozzle to the X-ray emission region near the neutron star. Consequently, no claim is made with respect to GX 301−2, but if the centroid of the mass transfer through the nozzle matched that of the X-ray luminosity, their calculations would imply a scale height of the primary atmosphere of a few percent of the effective Roche lobe radius. It is unclear if this model would reproduce other characteristics of GX 301−2's temporal variability, such as the relative intensities of "bright" and "mean" levels.

Since the spectra of the "bright" levels closely resemble those of the "mean" levels, the emission process responsible for the flaring during the "bright" levels is most probably the same one responsible for the "mean" flux. This in turn indicates that the flaring may be associated with either storing and dumping of matter that would have otherwise flowed smoothly to the emission site or with inhomogeneities in the wind. The latter effect has been addressed previously (Lucy 1982) in attempts to reconcile X-ray observations of single O stars with wind theory. For these stars the acceleration of the stellar wind is unstable and shocks form in the wind. These shocks then result in highly variable wind speeds and densities, which could cause the observed flaring in GX 301−2 (S. Owocki 1986, private communication). On the other hand, Makino, Leahy, and Kawai (1985) studied the correlation of the Fe line near 6–7 keV with inferred column density, and concluded that the variability they observed cannot be due to increases in the local density, but must be due to large-scale mass transfer.

IV. CONCLUSIONS

HEAO 1 observations of GX 301-2 through two complete 41.5 day binary cycles in the range 13–170 keV have shown the flux to increase about an order of magnitude from the mean on a daily average near periastron and to decrease about a factor of 2 near phase 0.2, presumably due to increased absorption/scattering within a few stellar radii of the primary. A smaller minimum near phase 0.7 is also present, which may be the result of attenuation by matter built up in the direction of the neutron star's motion. The X-ray spectrum is relatively unaffected by either orbital phase or flaring near periastron. The brightening near periastron lasts about 4 days (10% of the binary period) and is centered just before periastron passage. Near periastron the detailed light curve shows flaring on hour time scales. A smoothly varying component may also be present near periastron.

Attempts at simple modeling the behavior of GX 301−2 by wind-driven accretion failed to arrive at a consistent set of parameters that would describe all aspects of the X-ray flux variability. This implies that the situation is more complicated than simple wind models assume, and that derived parameters from such simple models may change when more sophisticated work is done. In particular, assumptions as to the velocity of the wind at the neutron star may have to include the effects on density and speed caused by shocks in the wind, the ambient X-ray heating of the wind, and the gravitational field of the neutron star.

Evidence for a spectral line feature was seen during one periastron passage, but could not be confirmed in any of the remaining data. Future hard X-ray missions, such as HEXE and XTE, will clearly have the sensitivity to measure such a feature, if it exists.

The authors would like to thank Drs. Jean Swank, Richard Kelley, Duane Gruber, Stan Owocki, and Noriake Shibazaki for their discussions. This research was supported by NASA grant NAG 8-499.

REFERENCES

Barlow, M. J., and Cohen, M. 1977, *Ap. J.*, **213**, 737.
Boyle, C. B. 1984, Ph.D. thesis, University of Glasgow.
Brown, J. C., and Boyle, C. B. 1984, *Astr. Ap.*, **141**, 379.
Castor, J. I., Abbott, D. C., and Klein, R. I. 1975, *Ap. J.*, **195**, 157.
Friend, D. B., and Castor, J. I. 1982, *Ap. J.*, **261**, 293.
Kelley, R., Rappaport, S., and Petre, R. 1980, *Ap. J.*, **238**, 699.
Lucy, L. B. 1982, *Ap. J.*, **255**, 286.
MacGregor, K. B., and Vitello, P. A. 1982, *Ap. J.*, **259**, 267.
Makino, F., Leahy, D. A., and Kawai, N. 1985, *Space Sci. Rev.*, **40**, 421.
Matteson, J. L. 1978, in *Proc. AIAA 16th Aerospace Science Meeting*, Huntsville, Alabama, Paper 78–35.
Okuda, T., and Sakashita, S. 1977, *Ap. Space Sci.*, **47**, 385.
Parkes, G. E., Mason, K. O., Murdin, P. G., and Culhane, J. L. 1980, *M.N.R.A.S.*, **191**, 547.
Robinson-Saba, J. L. 1983, Ph.D. thesis, University of Maryland.
Swank, J. H., Becker, R. H., Boldt, E. A., Holt, S. S., Pravdo, S. H., Rothschild, R. E., and Serlemitsos, P. J. 1976, *Ap. J.* (*Letters*), **209**, L57.
Warwick, R. S., Watson, M. G., and Sims, M. R. 1981, *Space Sci. Rev.*, **30**, 461.
Watson, M. G., Warwick, R. S., and Corbet, R. H. D. 1982, *M.N.R.A.S.*, **199**, 915.
White, N. E., and Swank, J. H. 1984, *Ap. J.*, **287**, 856.

RICHARD E. ROTHSCHILD and YANG SOONG: Center for Astrophysics and Space Sciences, C-011, University of California, San Diego, La Jolla, CA 92093